Model-based inference and classification of immunological control mechanisms from TKI cessation and dose reduction in CML patients

Tom Hähnel, Christoph Baldow, Joëlle Guilhot, François Guilhot, Susanne Saussele, Satu Mustjoki, Stefanie Jilg, Philipp J. Jost, Stephanie Dulucq, François-Xavier Mahon, Ingo Roeder, Artur C. Fassoni, Ingmar Glauche

Supplementary figures

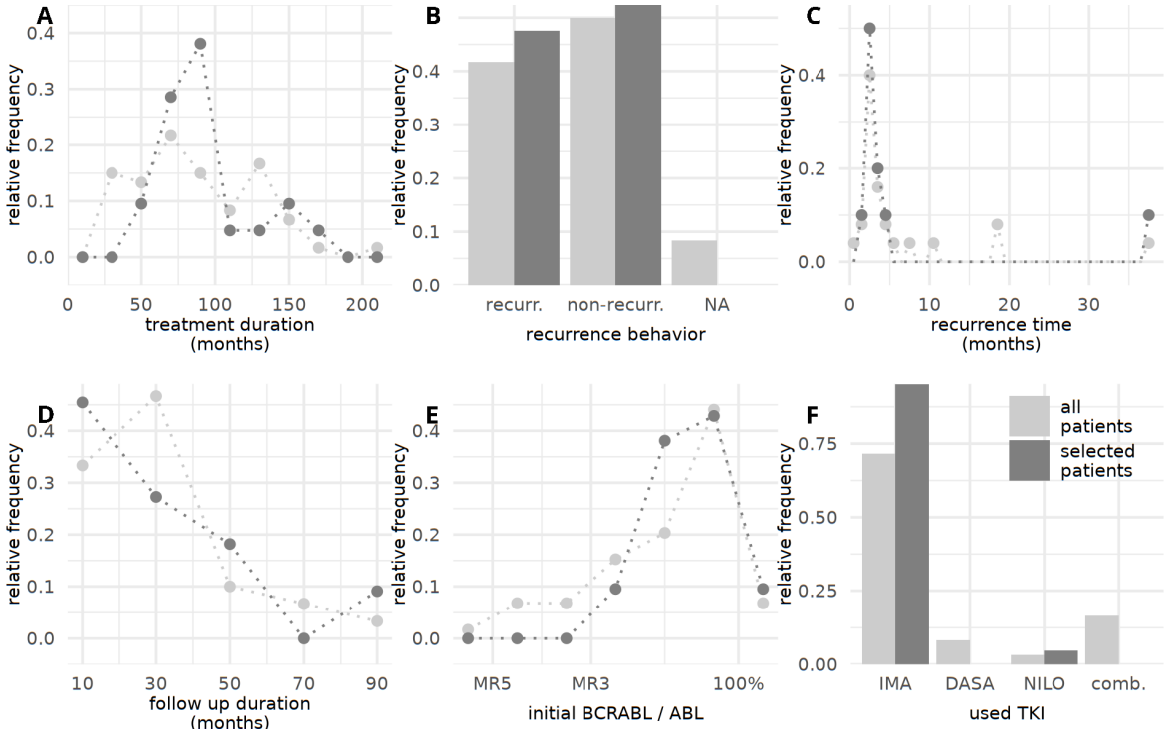

Fig. S1 Clinical characteristics of original and selected patients

A-F: Comparison of selected patients (dark grey, n =21) and all patients (light gray, n=60). The y axis depicts the relative frequency. **A**: Treatment duration until cessation. **B**: Relative frequency of recurring and non-recurring patients after stopping TKI treatment. NA indicates missing information about recurrence behavior of the patient. **C**: Time until recurrence after treatment stop. Recurrence is defined as loss of MMR (0.1% *BCR-ABL1/ABL1*) or initiation of re-treatment. **D**: Follow up duration for non-recurring patients after treatment cessation. **E**: Initial *BCR-ABL1* levels. Patients with initial *BCR-ABL1/ABL1* measurements below MR3 have been excluded. **F**: Drug used (DASA=Dasatinib, IMA=Imatinib, NILO=Nilotinib, comb.=combination therapy).

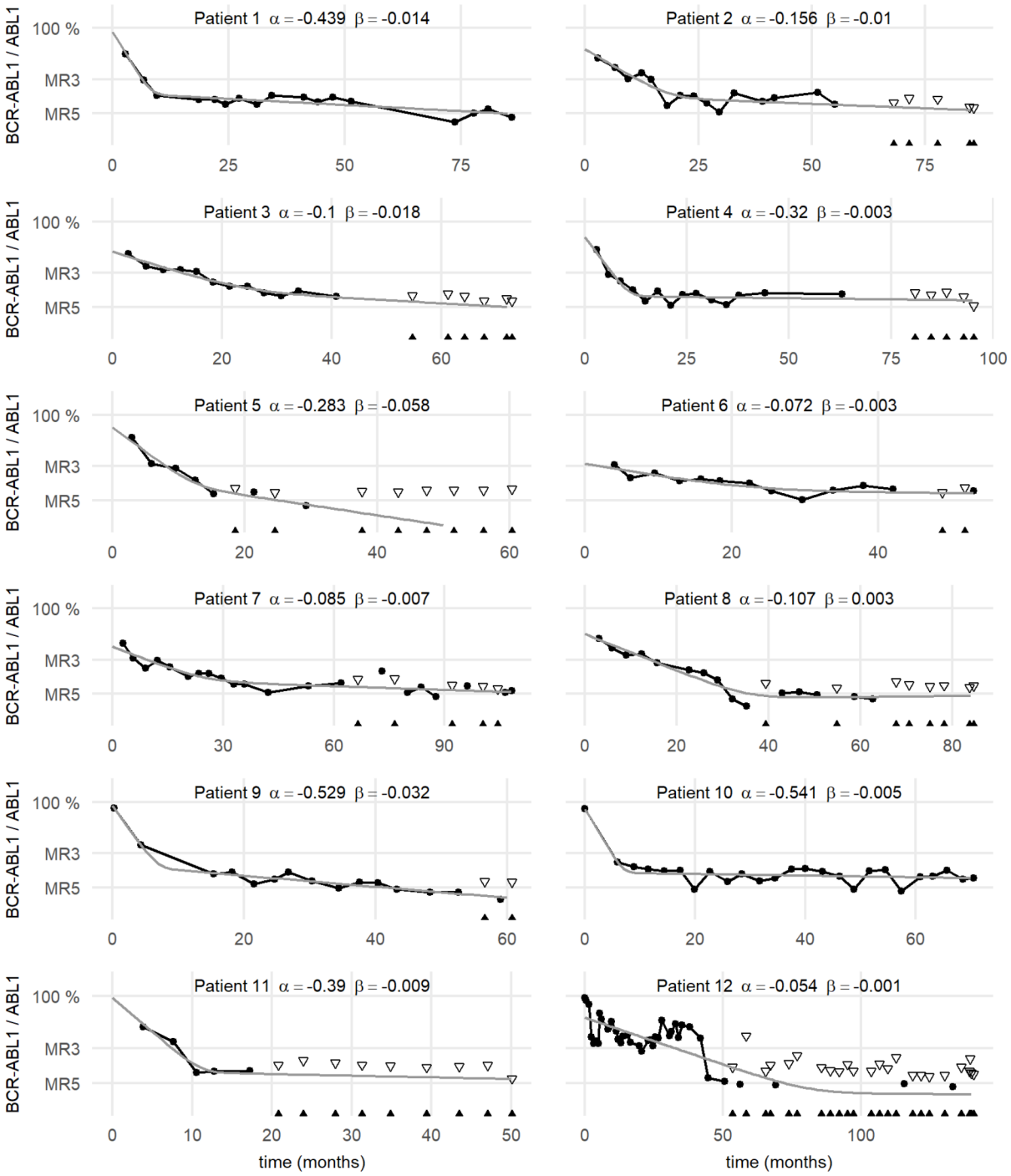

Fig. S2 clinical data with corresponding bi-exponential fits (1)

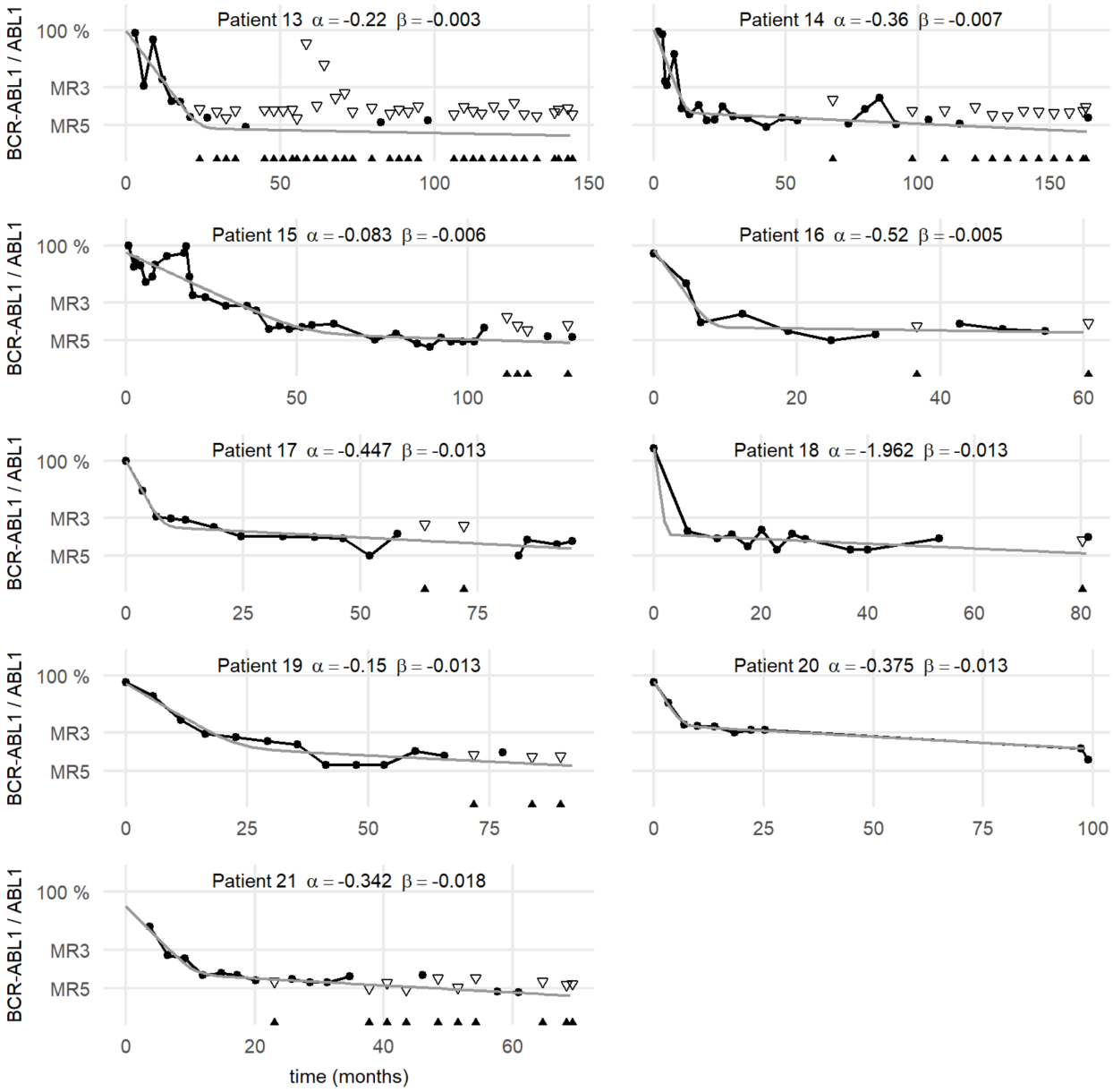

Fig. S2 clinical data with corresponding bi-exponential fits (2)

Clinical data and corresponding bi-exponential fits for the 21 selected patients prior to treatment cessation (heading contains estimated α and β slopes of the fit in units of log10(*BCR-ABL1/ABL*) change per month). *BCR-ABL1/ABL1* measurements are shown as black dots. Left-censoring is applied for measurements with undetectable *BCR-ABL1/ABL1* levels (see [1]), for which an upper bound is calculated based on the abundance of the reference gene (log10(3/copies of reference gene); see [5]).

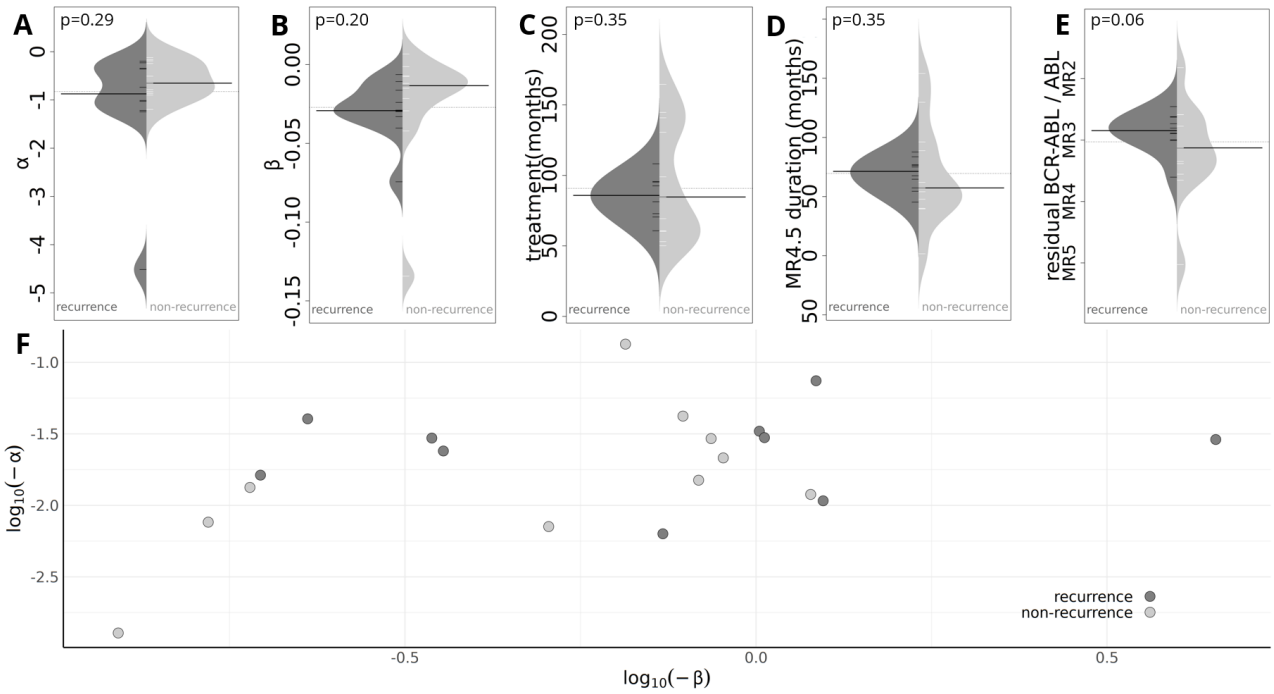

Fig. S3 No major differences of the *BCR-ABL1* decline characteristics between recurring and non-recurring patients

Comparison of recurring (dark grey) and non-recurring (light grey) patients by analyzing the clinical data and *BCR-ABL1* time courses before treatment stop. P-values of the corresponding Kolmogorow-Smirnov tests are shown **A/B**: Steepness of the first, fast decline (α) and the second, slow decline (β) estimated by fitting the patient data to the bi-exponential model. **C**: Treatment duration before cessation. **D**: Time of deep molecular remission (DMR, reduction of 4.5 logs from the baseline) while treated, **E**: *BCR-ABL1* levels at cessation estimated using the corresponding individual bi-exponential fits. **F**: Distribution of α and beta for recurring and non-recurring patients. Overall, we detected no obvious differences between the recurring and non-recurring patient groups. The 21 individual bi-exponential fits are shown in Figure S2.

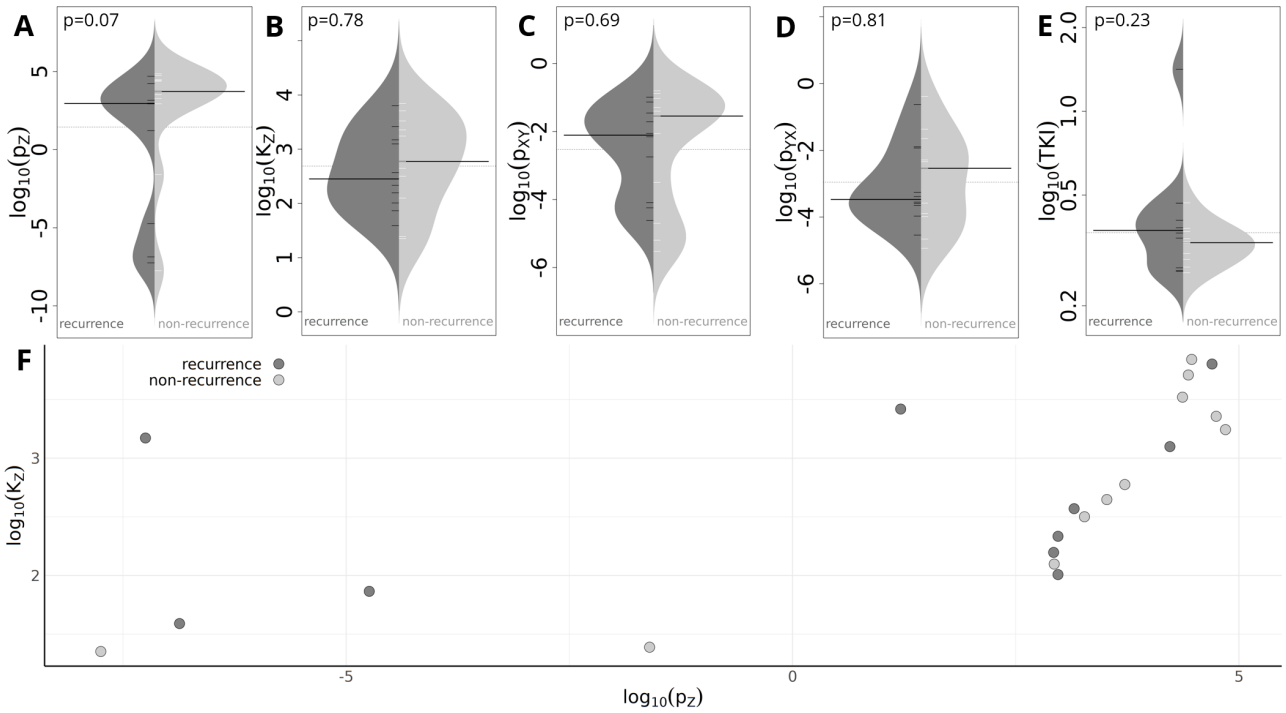

Fig. S4 Estimated model parameters for recurring and non-recurring patients obtained from fitting the mathematical model to measurements *before* cessation (fitting strategy II)

A-E: Comparison of the parameter estimations for recurring (dark grey) and non-recurring (light grey) patients, estimated by fitting the immune system model to the initial *BCR-ABL1* time courses *before* treatment cessation (fitting strategy II). P-values of the corresponding Kolmogorow-Smirnov tests are shown. **F**: Bivariate analysis of the immune system parameters p_z and K_z for recurring (dark grey) and non-recurring (light grey) patients. Overall, we detected no obvious differences between the recurring and non-recurring patient groups.

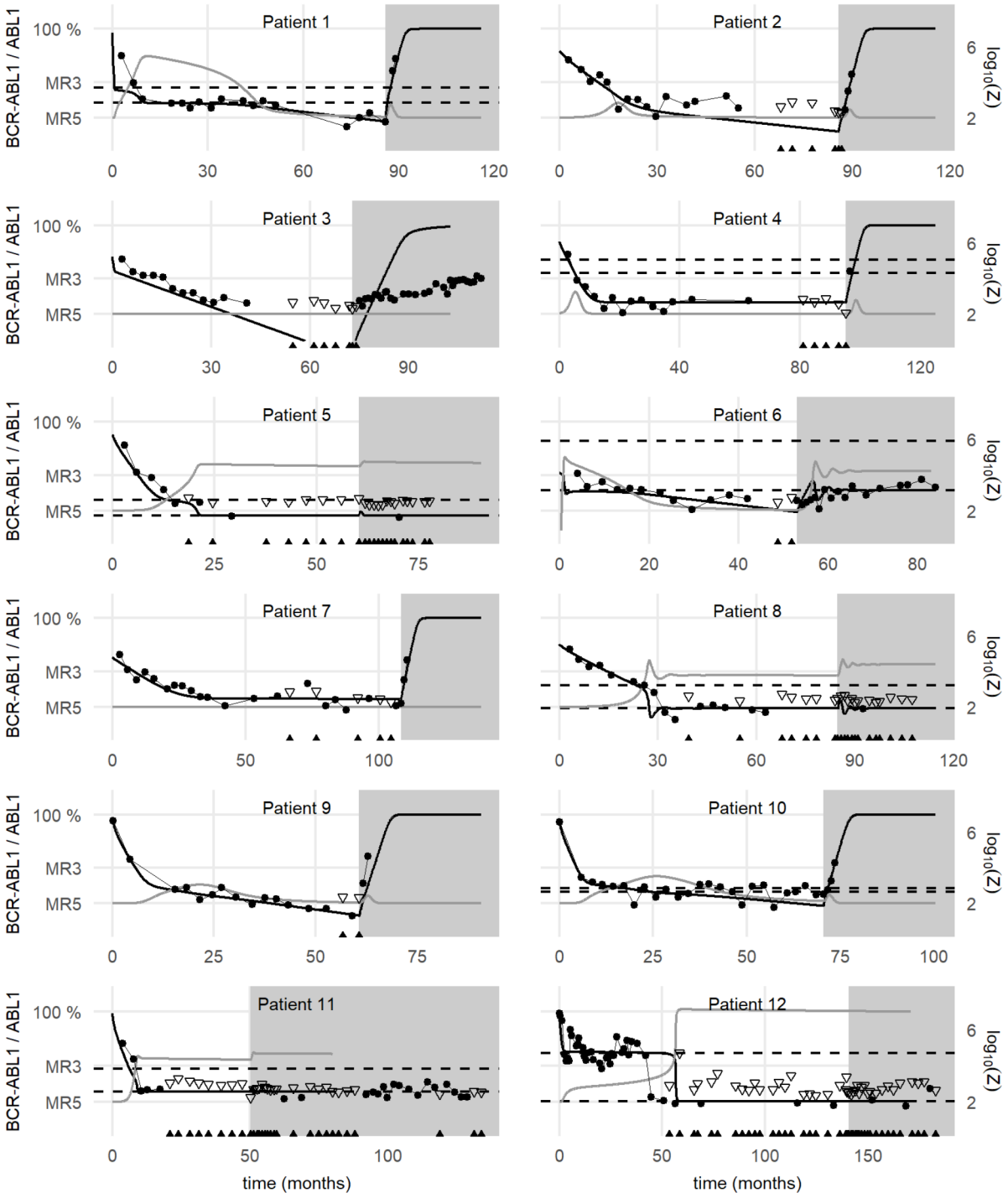

Fig. S5: clinical data with corresponding immune system model simulations (1)

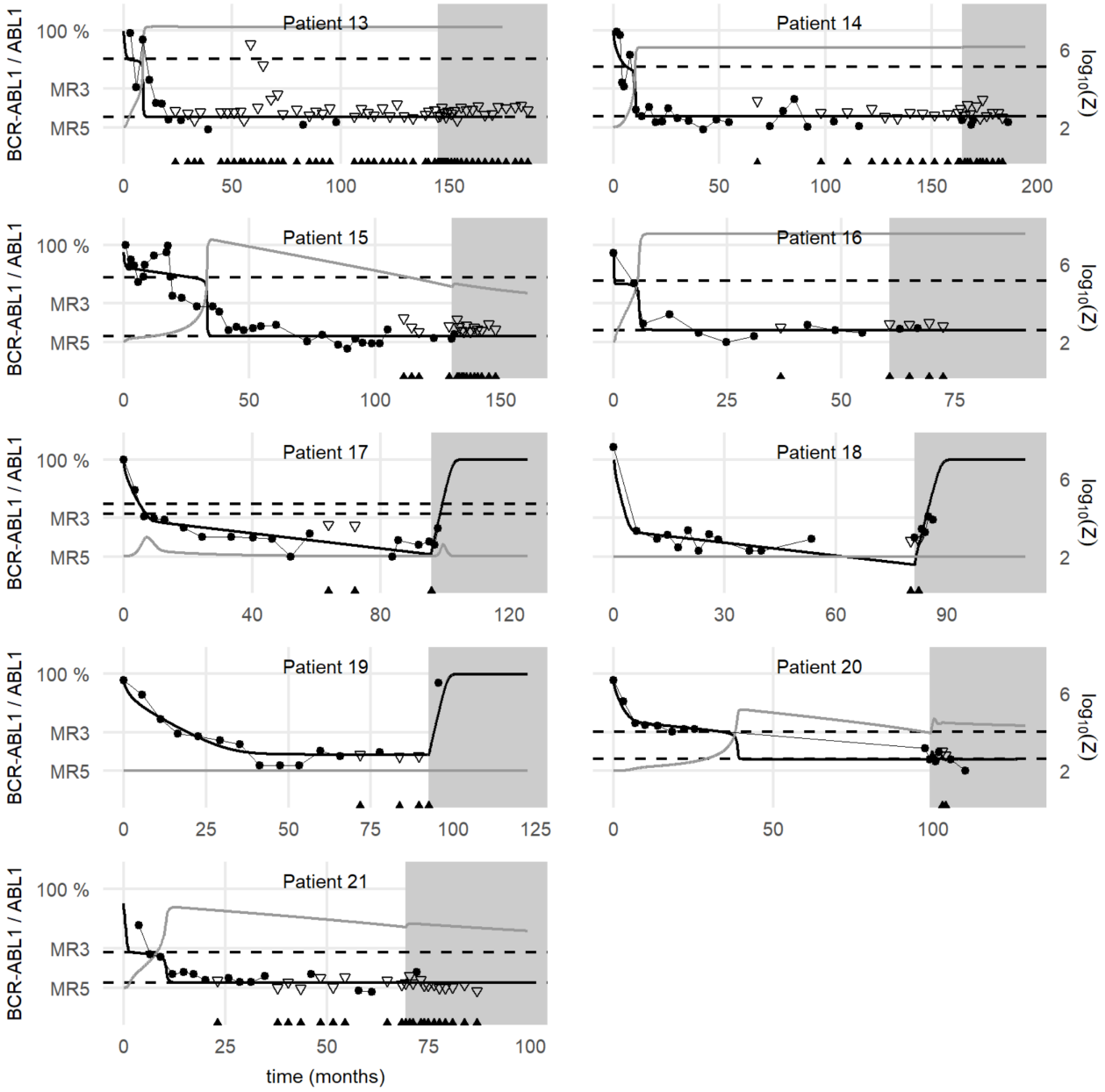

Fig. S5: clinical data with corresponding immune system model fits (2)
Clinical data and corresponding immune model simulations of the 21 selected patients obtained by using fitting strategy III. *BCR-ABL1* measurements are shown as black dots or triangles (see Fig. S2). The grey shaded area indicates the time period after treatment cessation. The immune window is located between the two dashed horizontal lines. Simulated *BCR-ABL1* values (black line) and corresponding relative numbers of immune cells (grey line) are shown on a logarithmic scale. The following fixed parameter values were used for all patients: K_Y=1e+06, m=1e-04, r_z=200, p_y=1.658, a=2. The remaining, individual estimated parameter can be obtained from Table S1.

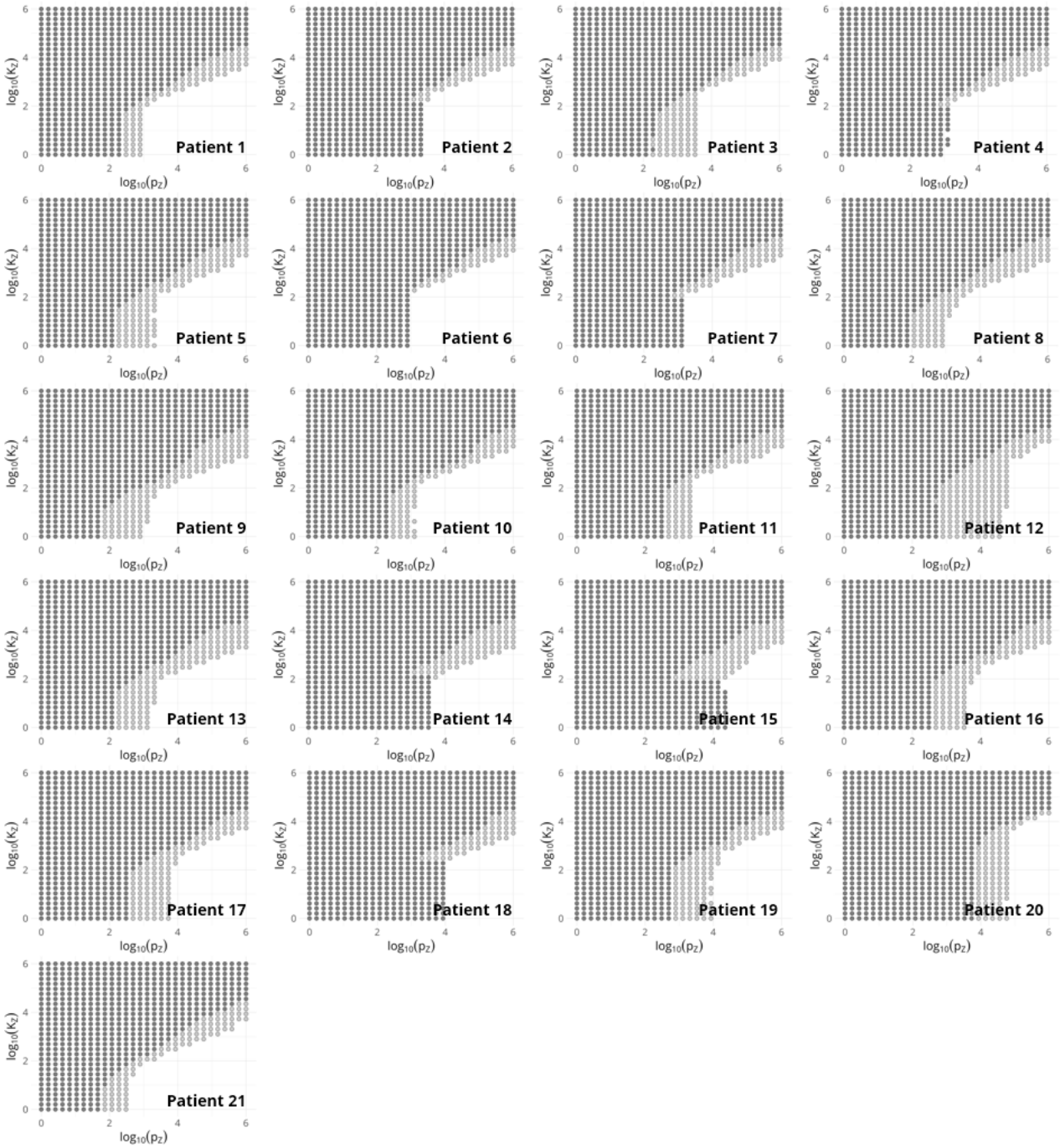

Fig. S6 predicted recurrence behavior depending on the immune parameters p_Z and K_Z. Predicted recurrence behavior for all 21 patients depending on the values of the immune parameters (p_z, K_z) taken within a predefined grid. The remaining free parameters (p_{XY}, p_{YX}, TKI) were obtained by using fitting strategy III. Only parameter estimations leading to sufficiently good fits are shown (i.e. with a residual sum of squares (RSS) less than twice the RSS of the best fit).

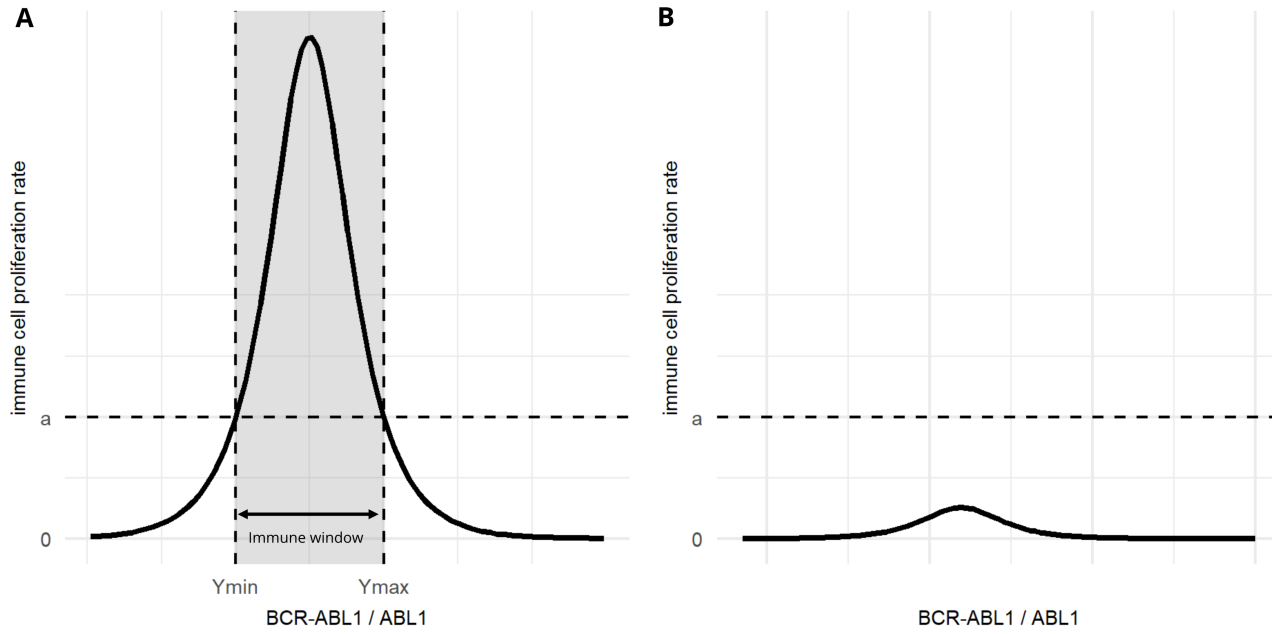

Fig. S7 immune window

The immune window (grey area between the vertical dashed lines) is defined as the range of leukemic cells for which the immune cell proliferation rate exceeds the immune apoptosis rate. The existence of the immune window depends on the individual values of the immunological parameter. Thus, it exists in patients with a *strong* or *weak* immune response (A) whereas patients with an *insufficient* immune response do not have an immune window (B).

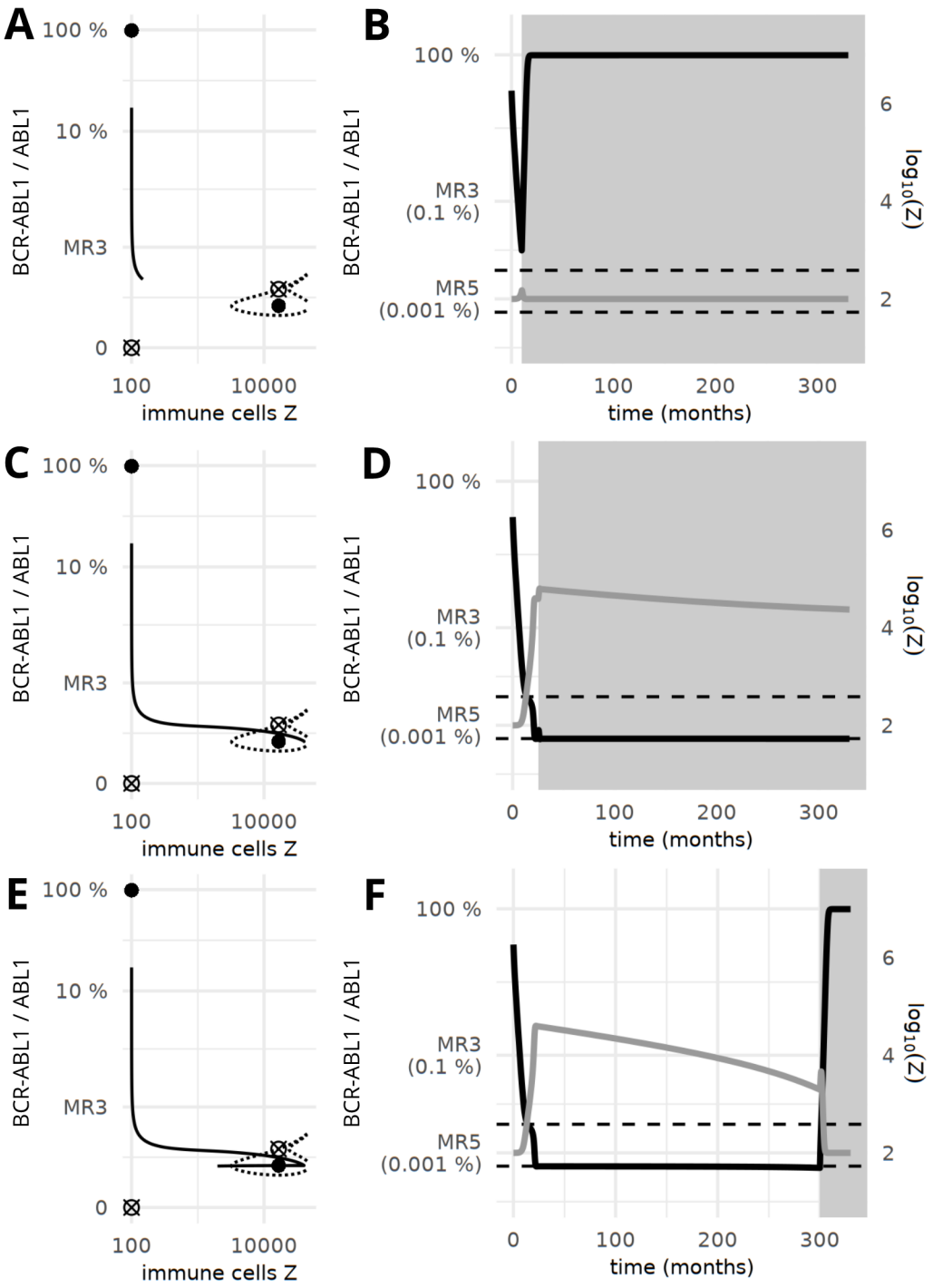

Fig. S8 Model predictions suggest that recurrences of patients with a weak immune response (class C) can be prevented by applying an *optimized treatment duration*.
Representation of the attractor landscapes with corresponding clinical data and simulation results of patient 5 for different treatment times obtained by fitting the immune model using fitting strategy III. **A/C/E**: The phase spaces are shown on the left side (see description of Fig. 4/5 for details) together with the trajectories of the number of leukemic cells and immune cells before stopping treatment (black solid lines). **B/D/F**: The time courses of the *BCR-ABL1/ABL1* and immune cells including the time after stopping treatment corresponding to each phase portrait are shown on the right side. The grey area indicates the time after treatment cessation. The immune window is depicted as the area between both horizontal dashed lines. Calculated *BCR-ABL1* values (black line) and corresponding relative number of immune cells (grey line) on a logarithmic scale are shown.

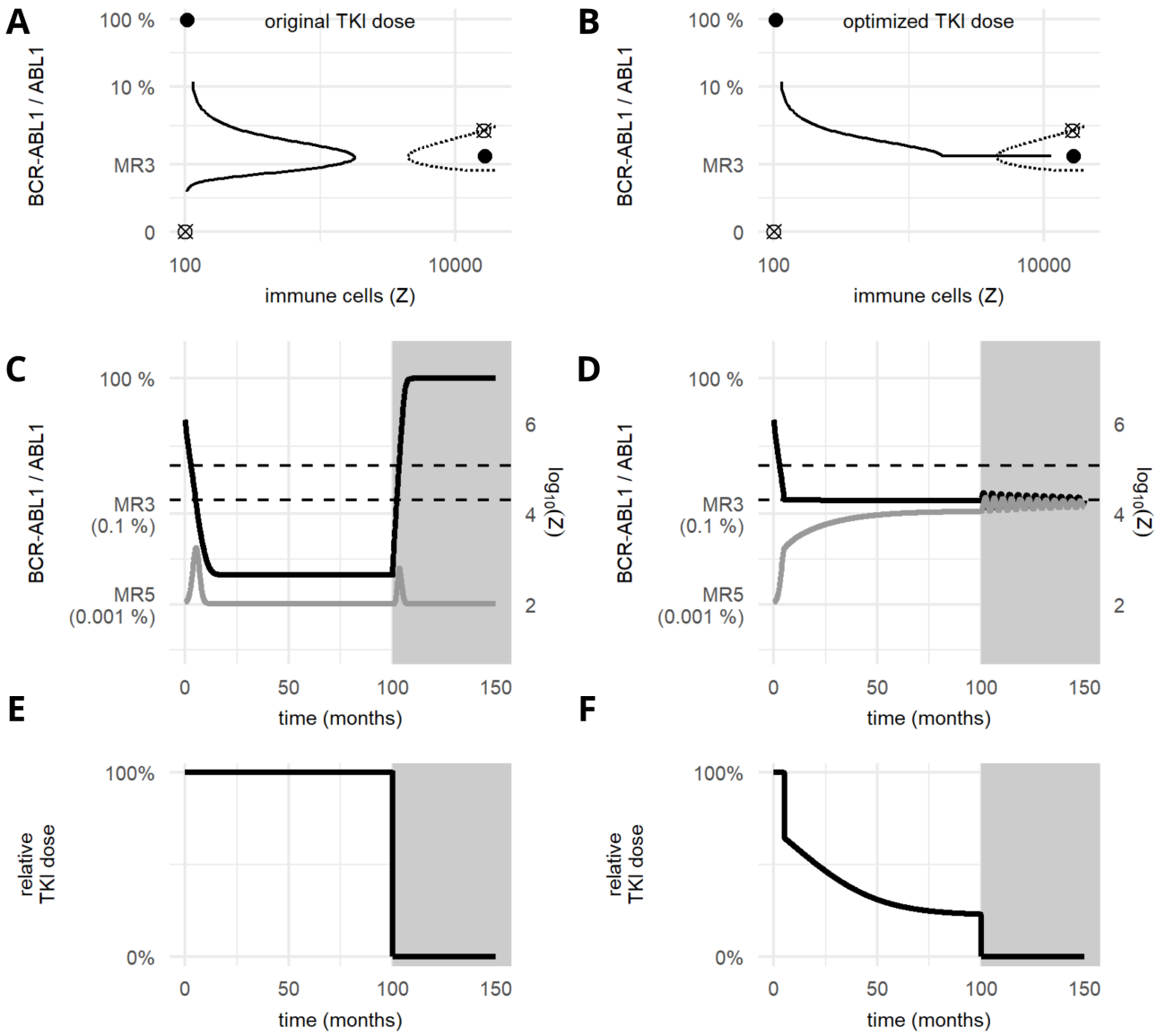

Fig. S9 Model predictions suggest that recurrences of patients with a weak immune response (class C) can be prevented by applying an *optimized treatment intensity strategy.*
The original treatment strategy using a constant value for the TKI intensity is shown on the left side. The optimized treatment approach using a treatment strategy which reduces the TKI dose when the lower limit of the immune window limit is reached is shown on the right side (see also Supplementary text). **A/B:** The phase portrait with the corresponding course of the leukemic cells and immune cells (see Fig. 4/5 for a detailed description). **C/D**: Depiction of the *BCR-ABL1/ABL1* and leukemic cell course. The grey area indicates the time after treatment cessation. The immune window is depicted as the area between both horizontal dashed lines. Calculated *BCR-ABL1* values (black line) and corresponding relative number of immune cells (grey line) of the model on a logarithmic scale are shown. **E**: The original treatment strategy applied in A/C. **F**: The optimized treatment approach using a treatment strategy which reduces the TKI dose when the lower limit of the immune window limit is reached (applied in B/D).